NUREG/CR-4998
LA-11117-MS

c. 3

Los Alamos National Laboratory is operated by the University of California for the United States Department of Energy under contract W-7405-ENG-36

The Seismic Category I Structures Program: Results for FY 1985

Los Alamos National Laboratory
Los Alamos, New Mexico 87545

NUREG/CR-4998
LA-11117-MS

RA

The Seismic Category I Structures Program: Results for FY 1985

Joel G. Bennett
Richard C. Dove*
Wade E. Dunwoody
Charles R. Farrar
Peggy Goldman

Manuscript submitted: August 1987
Date published: December 1987

Prepared for
Division of Engineering
Office of Nuclear Regulatory Research
US Nuclear Regulatory Commission
Washington, DC 20555

NRC FIN No. A7221

*Consultant at Los Alamos. 0764 CR65, Del Norte, CO 81132.

Los Alamos
Los Alamos National Laboratory
Los Alamos, New Mexico 87545

CONTENTS

FIGURES

TABLES

THE SEISMIC CATEGORY I STRUCTURES PROGRAM: RESULTS FOR FY 1985

by

Joel G. Bennett, Richard C. Dove, Wade E. Dunwoody,
Charles R. Farrar, and Peggy Goldman

ABSTRACT

In FY 1985 a new effort was begun to resolve an issue that became the "stiffness difference issue." This issue came about from reporting the results from testing both isolated shear walls and box-like shear deformation-dominated scale models that showed a consistent reduction in structural stiffness measured experimentally. This structural stiffness was different from that which would be calculated analytically at loads associated with operating basis earthquake levels. Several possible explanations were proposed for the experimental/analytical difference (most likely attributable to cracking of the concrete models). Possibilities are microcracking at very low loads, microconcrete effects, such as shrinkage cracks, unaccounted for dynamic effects in the analyses, and low stress level, low-cycle, fatigue degradation of microconcrete properties. A new configuration was proposed by the Technical Review Group (TRG) for this program and, in FY 1985, a prototype structure was designed. A 1/4-scale microconcrete model of the prototype structure was constructed and tested. This report details that investigation, but it does not report the resolution of the "stiffness difference" issue, an investigation that was ongoing at the end of FY 1985.

I. INTRODUCTION

The Seismic Category I Structures Program is being carried out at the Los Alamos National Laboratory under sponsorship of the U.S. Nuclear Regulatory Commission (NRC), Office of Nuclear Regulatory Research. The program has the objective of investigating the structural dynamic response of Seismic Category I reinforced concrete structures (exclusive of containment) that are subjected to seismic loads beyond their design basis. The program, as originally conceived, is a combined experimental/analytical investigation with heavy emphasis on the experiment component to establish a good data base. A number of meetings and interactions with the NRC staff has led to the following set of specific program objectives:

1. Address the seismic response of reinforced concrete Category I structures, other than containments.

2. Develop experimental data for determining the sensitivity of structural behavior of Category I structures in the elastic and inelastic response range to variations in configuration, design practices, and earthquake loading.

3. Develop experimental data to enable validation of computer programs used to predict the behavior of Category I structures during earthquake motions that causes elastic and inelastic response.

4. Identify floor response spectra changes that occur during earthquake motions that cause elastic and inelastic structural response.

5. Develop a method for representing damping in the inelastic range and demonstrate how this damping changes when structural response goes from the elastic to the inelastic ranges.

6. Assess how shifts in structural frequency affect plant risk.

The outstanding feature of the typical structure under investigation is that shear rather than flexure is dominant; that is, the ratio of displacement values, calculated from terms identified with shear deformation, to the values contributed from bending deformation is one or greater. Thus these buildings are called "shear wall" structures. The background of the program will be briefly summarized below.

The Seismic Category I Structures Program began in FY 1980 with an investigation that identified the typical nuclear shear wall structure and its characteristics (stiffnesses, frequencies, etc.). A combined experimental/

analytical plan for investigation of the dynamic behavior of these structures was laid out as described in Ref. 1. During the first phase, the program concentrated on investigating isolated shear wall behavior using small models (1/30-scale) that could be economically constructed and tested both statically and dynamically. Also during this phase of the program, a Technical Review Group (TRG) of nationally recognized seismic and concrete experts on nuclear civil structures was established to both review the progress and make recommendations regarding the technical direction of the program. The recommendations of this group have been evaluated in light of the needs of the USNRC and, when possible, have been carefully integrated into the program.

Following the isolated shear wall phase, the program began testing and evaluating 3-D box-like model structures. It was recognized from the outset that scale model testing of concrete structures is a controversial issue in the U.S. civil engineering community. Therefore, in addition to the testing of small-scale test structures, a task of demonstrating scalability of the results to prototype structures was initiated. The details and results of these investigations are reported in Refs. 2-5.

This document reports the work carried out in FY 1985 as part of an effort to address the specific objectives. As such, it is organized as follows: Section II summarizes the status of the program at the end of FY 1984. Section III summarizes the results of both a 1/42- and a 1/14-scale model test of an auxiliary building, tasks that were in progress at the end of FY 1984. Section IV reports the work and meetings that led to the design of the TRG structures. Section V reports the design, testing, and results of the first 1/4-scale TRG model. Finally, Section VI gives the conclusions and recommendations as a result of the work for FY 1985.

II. STATUS OF THE SEISMIC CATEGORY I STRUCTURES PROGRAM AT THE END OF FY 1984.

The Seismic Category I Structures Program basically had finished a phase of a program plan that tested, either seismically or statically, box-like microconcrete models that represented two types of idealized structures, a diesel generator building and an auxiliary building. Two different scales, (1/30, 1/10) and (1/42, 1/14), of these buildings were used (with 1-in. and 3-in. walls), and the number of stories varied from one to three. Furthermore, the scaling was planned so that all 1/30- and 1/42-scale models were Case II models of the prototype structures. For the details, see Ref. 6 and Appendix C of Ref. 7 of for a complete discussion on the scaling laws and their use in this program. The 1/42-scale model test was just completed and the 1/14-scale model was being constructed for testing in December, but the basic results of all microconcrete model tests that began to address the program objectives were reported at the NRC-sponsored 12th Light Water Reactor Safety Information Meeting (LWRSIM) on October 22, 1984. The TRG met in conjunction with this meeting to review these results.

Although a number of results on items such as aging (cure time) and effect of increasing seismic magnitude had been reported, two important and consistent conclusions came out of the data from these test. First, the scalability of the results was illustrated both in the elastic and inelastic range. Second, the so-called "working load" secant stiffness of the models was lower than the computed uncracked cross-sectional values by a factor of about 4. The term "working load" is meant to be a load that produces stress levels equivalent to the design basis earthquake.

During the review, the TRG pointed out the following factors:

1. Design of prototype nuclear plant structures is normally based upon an uncracked cross-section strength-of-materials approach that may or may not use a "stiffness reduction factor" for the concrete. However, if such a factor is used, it is never as large as 4.
2. Although the structures themselves appear to have adequate reserve margin (even if the stiffness is only 25% of the theoretical), any piping and attached equipment will have been designed using inappropriate floor response spectra.
3. Given that a nuclear plant structure designed to have a natural response of about 15 Hz really has a natural frequency of 7 Hz (corresponding to a reduction in stiffness of 4), and allowing further that the natural frequency will decrease because of degrading stiffness, the natural response of the structure will shift well down into the frequency range where an earthquake's energy content is the largest. This shift will result in increased amplification in the floor response spectra at lower frequencies, and this fact potentially has impact on the equipment and piping design response spectra and on margins of safety.

Note that all three points are related to the difference between measured and calculated stiffnesses of these structures.

Having made these observations, several questions now arose. Does the previous experimental data taken on microconcrete models represent data that would be observed with prototype structures? What is the appropriate value of the stiffness that should be used in design and for component response spectra computations in these structures? Should it be a function of load level? Have the equipment and piping in existing buildings been designed to inappropriate response spectra? What steps should be taken to evaluate this reduced stiffness for existing structures?

Thus, the primary program emphasis starting in FY 1985 was to ensure credibility of previous experimental work by beginning to resolve the difference between the analytical and theoretical stiffness that came to be called the "stiffness difference" issue. The TRG for this program believed that this important issue should be addressed before the program objectives could be accomplished.

It was agreed that a series of credibility experiments would be carried out using both large- and small-scale structures. For the large-scale structure, the TRG set limitations on the design parameters. Their recommended "ideal" structure characteristics, in order of decreasing priority, were as follows:

1. Maximum predicted bending and shear mode natural frequency $\leq$30 Hz.
2. Minimum wall thickness = 4 in.
3. Height-to-depth ratio of shear wall $\leq$1.
4. Use actual No. 3 rebar for reinforcing.
5. Use realistic material for aggregate.
6. Use 0.1% to 1% steel (0.3% each face, each direction ideally).
7. Use water-blasted construction joints to ensure good aggregate frictional interlock.

It was further agreed that the best plan would be to build two of these structures as nearly identical as possible. To compare the results from these tests with previously obtained data, one model should be tested quasistatically and cyclically to failure and the second model should be tested dynamically.

This summary of the program status defines the situation as it existed at the end of FY 1984 and through the early part of FY 1985.

III. SUMMARY OF THE 1/42-AND 1/14-SCALE MODEL AUXILIARY BUILDING EXPERIMENTS

The 1/42-scale model (1-in.-thick walls) auxiliary building experiment was completed in FY 1984, but data reduction was carried out in FY 1985. The 1/14-scale model (3-in.-thick walls) construction began in FY 1984, with the testing and data reduction carried out in FY 1985. Reference 7 is a topical report that completely details these tests, but because the tests were part of the FY 1985 effort, the results will be summarized here. The TRG had suggested that a geometry different from the diesel generator building be tested maintaining, however, the 1-in. and 3-in. wall thickness. The reasoning behind the suggestion was to exclude the possibility that the results were geometry-dependent. After a study of actual plants, the auxiliary building was chosen for modeling.

The idealized prototype auxiliary building of interest was three stories. Its dimensions and those of the scale models are shown in Fig. 1. The basic construction materials (microconcrete and wire mesh or scaled deformed bars) were the same for this model as they were for the 1/30- and 1/10-scale models of Ref. 5. Details of construction and testing are contained in Ref. 7. Testing of the 1/42-scale model was done at the Sandia National Laboratory (SNL)

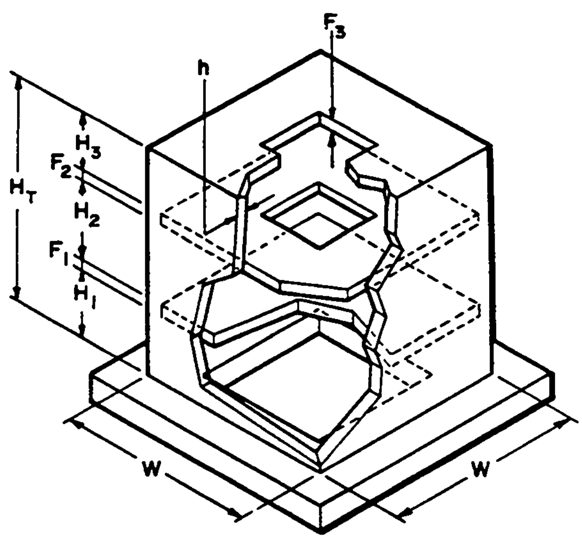

	h, F_1, F_2, F_3	W	H_1, H_2, H_3	Wt/STORY* (lb)
1/42 SCALE	1 in.	26 in.	10 in.	140
1/14 SCALE	3 in.	78 in.	30 in.	3780
PROTOTYPE	42 in.	1092 in.	42 in.	10,372,000

*BASE NOT INCLUDED

Fig. 1. Idealized three-story auxiliary building: models and prototype.

and the 1/14 scale was transported to the Construction Engineering Research Laboratory (CERL) at Champaign, IL.

The test plan at SNL for the 1/42-scale model was completed without mishap. However, shaker control problems caused unrecorded table excursion as well as two 2-g pulses (0.4 g on the prototype) to be accidentally applied during shaker warm-up phase at CERL. This severely damaged the 1/14-scale model before the test plan began. The test plan was completed on the damaged model, but the data clearly show that the 1/14-scale structure no longer is modeled by the 1/42-scale structure. Figure 2 illustrates these results in terms of the two structures' first-mode frequency plotted vs peak seismic excitation. The effect of cummulative damage on the structures is evidenced by the increasingly downward shift in first-mode frequency, indicating degrading stiffness as additional seismic events of increasing magnitude are applied. All results in Fig. 2 are scaled to the prototype structure. To obtain actual

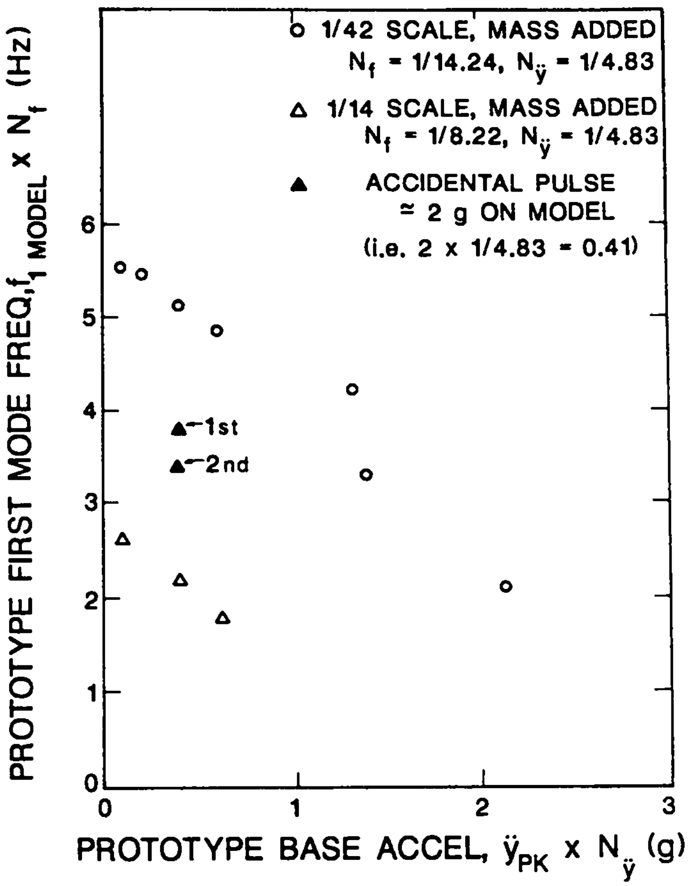

Fig. 2. First-mode frequency vs peak acceleration.

model results, the scale factors shown in Fig. 2, presented as the ratio of prototype to model, must be used. For example, for 5 Hz, predicted on the ordinate (and thus on the prototype) of Fig. 2, and for the 1/42-scale model, $N_f = f_p/f_m = 1/14.24$, $f_p = 5\text{Hz}$, $f_m = 14.24 \times 5$ Hz. Thus, $f_m = 71.2$ Hz was actually measured on the model. If the 1/42- and 1/14-scale models had been models of each other for these tests, the data should all fall along the same line.

Prior to accidental damage of the 1/14-scale structure, the 1/14-scale model fundamental frequencies (f_1, f_2, and f_3), as a bare model (no added mass), were measured using a random broad band 0.5-g low-level (0.1-g on the prototype) forcing function. Table I shows a comparison of the analytically computed frequencies, those predicted from the 1/42-scale test, and the measured values. This table indicates that, before accidental damage, the 1/14-scale model was predicted reasonably well by the 1/42 scale, but it was below those values that would be computed analytically. This result confirms the same low-level reduced stiffness effects observed in the prior tests of Refs. 4 and 5.

To illustrate this effect further, Table II summarizes the reduced stiffness (K) effect for both of these model structures, as measured initially by applying a 0.5-g (0.1-g on the prototype) broad band random base input signal. These data will be compared with other data from this program in the next section of this report. Details of the computations are given in Ref. 7, but basically, the frequencies were computed from modeling the structures as three-floor lumped mass systems, with shear and bending spring stiffnesses between floors included in the computation as determined from an uncracked strength-of-materials approach.

TABLE 1

COMPARISON OF INITIAL FUNDAMENTAL FREQUENCIES

1/14-SCALE MODEL

f_1, f_2, f_3 predicted from the 1/42 scale test data (Hz)	f_1, f_2, f_3 measured during the test (Hz)	f_1, f_2, f_3 analytically predicted (Hz)
62	57	149
201	172	408
303	299	587

TABLE II

COMPARISON OF ANALYTICAL AND MEASURED INITIAL FREQUENCIES AND STIFFNESSES FOR THE 1/42- AND 1/14-SCALE MODEL AUXILIARY BUILDINGS

	Computed Model Frequencies f_1, f_2, f_3 (Hz)	Measured Model Frequencies f_1, f_2, f_3 (Hz)	$\frac{f_{meas}}{f_{comp}}$	$\frac{k_{meas}}{k_{comp}} = \left(\frac{f_{meas}}{f_{comp}}\right)^2$
1/42-scale	435	187	0.43	0.18
bare model	1185	605	0.51	0.26
	1705	910	0.53	0.28
1/42-scale	156	80	0.51	0.26
model with	425	236	0.56	0.31
added mass	609	327	0.54	0.29
1/14-scale	149	57	0.38	0.14
bare model	408	172	0.42	0.18
	587	299	0.51	0.26

With the exception of demonstrating a clear scale model relationship between these two structures, the basic findings in the previous 1/30- and 1/10-scale model tests reported in Ref. 5 are strongly supported by these two tests.

IV. REVIEW OF PREVIOUS TESTS

Following the reaction to the work reported to the TRG at the 12th LWRSIM, a complete review of the methods used and values determined for reporting stiffnesses of these structures was undertaken. This review pointed out that all static stiffnesses that had been reported in the past had been determined as being the secant stiffnesses for first-indicated cracking on the load displacement curve. Figure 3 illustrates this determination. The load displacement curve for test structure 3D-2, which was a diesel generator building model tested in the transverse (short) direction under a monotonically increasing load is shown. Cracking of the structure is indicated by a horizontal deflection with no increase in loading. First cracking of this structure occurred at P_c = 5210 lb, with the deflection (after cracking) reading of 0.0096 in. This method of computing stiffness would indicate a value of

$$K = \frac{5210 \text{ lb}}{0.0096 \text{ in.}} = 0.54 \times 10^6 \text{ lb/in.}$$

However, if the stiffness is evaluated on the basis of being the secant modulus through a point corresponding to 50% of the ultimate strength of the structure (ie. a design "working" load), then

$$K = \frac{4470 \text{ lb}}{0.0059 \text{ in.}} = 0.76 \text{ lb/in.}$$

The stiffness computed in this manner was defined as the "working" load stiffness. The stiffness from dynamic tests was determined indirectly by measuring the lowest-mode natural frequency and by using the relationship that

$$\left(\frac{k_{\text{measured}}}{k_{\text{theoretical}}}\right) = \left(\frac{f_{\text{measured}}}{f_{\text{theoretical}}}\right)^2 .$$

The method for determining the lumped mass theoretical model will be described. For the theoretical value of stiffness, an uncracked strength-of-materials approach was used. The formula, including both flexural and shear deformation, is

$$K = \frac{GA_e}{h}\left(\frac{\alpha}{4 + \alpha}\right) ,$$

where

G = the concrete shear modulus,
h = the story height,
A_e = the effective shear area,
α = $12\, E_c I/GA_e h^2$,
E_c = the concrete elastic modulus, and
I = the section moment of inertia about the neutral axis for bending.

The effective shear area is the area for shear flow (the "web" area) in the direction of loading. For the 1/30-scale diesel generator buildings (dimensions are shown in Fig. 4) tested transversely, this area is

$$A_e = 2 \text{ walls } (10 \text{ in./wall})(1 \text{ in.}) = 20 \text{ in.}^2$$

In these calculations, the Poisson's ratio was always taken to be

$$\nu = 0.2,$$

so that G and E are related by

$$G = E/2\,(1 + \nu) \quad = \quad E/2.4.$$

Thus, for the 3D-2 experiment with

$$h = 7.25 \text{ in.}$$

$$I = 817.33 \text{ in.}^4$$

then, $K = 0.98\ E_c$.

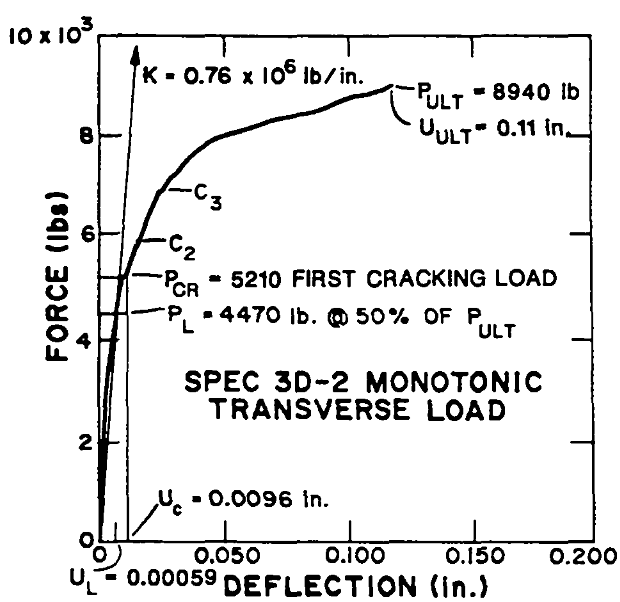

Fig. 3. Load deformation curve for experiment 3D-2.

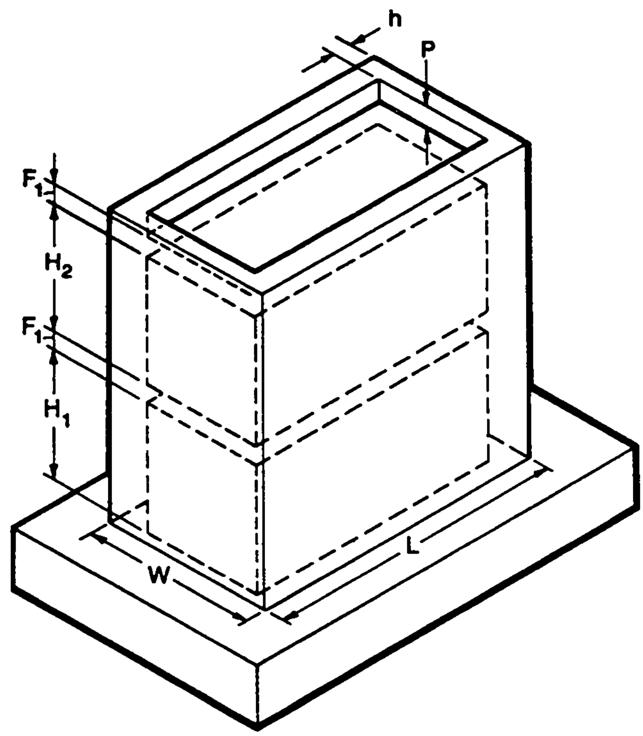

	h, F_1, F_2	W	L	H_1 & H_2	P	Wt/STORY *
1/30 SCALE	1 in.	10 in.	18 in.	7.25 in.	1 in.	47.7 lb
1/10 SCALE	3 in.	30 in.	54 in.	21.75 in.	3 in.	1286 lb
PROTOTYPE	30 in.	25 ft	45 ft	18.125 ft	30 in.	1,286,000 lb

*BASE NOT INCLUDED

NOTE: 1 in. = 25.4 mm, 1 ft = 0.305 m, 1 lb = 4.45 N

Fig. 4. Idealized two-story diesel generator building: models and prototype.

The TRG indicated that the initial stiffnesses of these structures would probably be incredible, if they were much less than one-fourth of this theoretical value. The review of all the 1/30 scale tests was carried out and each test is plotted on Figs. 5 and 6 for the transverse and the longitudinal directions, respectively. The theoretical limit and one-fourth of this limit are also shown on these figures. As can be seen, nearly all tests fall within these limits. E_c was taken to be 57000 $\sqrt{f'_c}$, in accordance with recommended civil engineering practice, where f'_c is the ultimate compressive strength of the concrete as determined from a standard cylinder test.

If all data are normalized by the uncracked theoretical value and plotted vs E_c, the reduced stiffness effect from all previous tests in this program can be shown on one graph, as in Fig. 7. This figure shows that the data

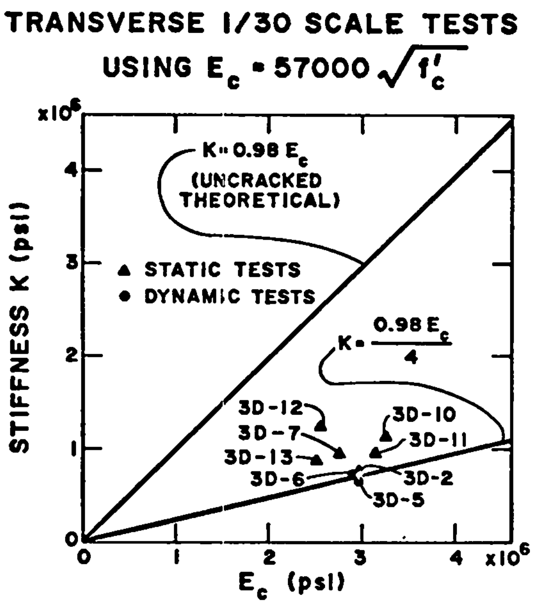

Fig. 5. Measured stiffness from the 1/30-scale tests on 3-D shear wall models tested in the transverse direction.

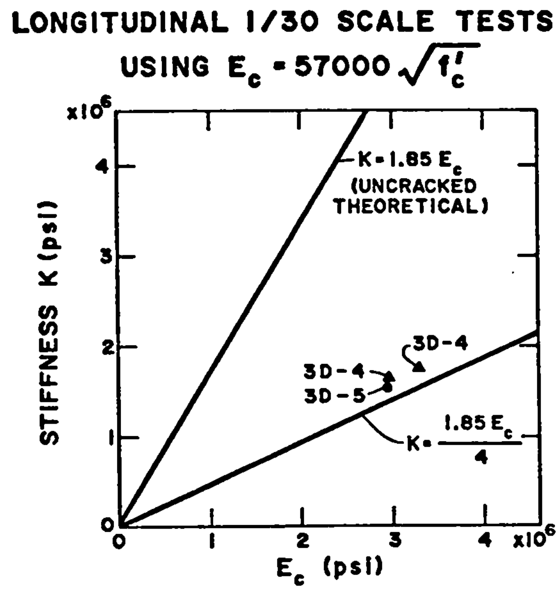

Fig. 6. Measured stiffness from the 1/30-scale tests on 3-D shear wall models tested in the longitudinal direction.

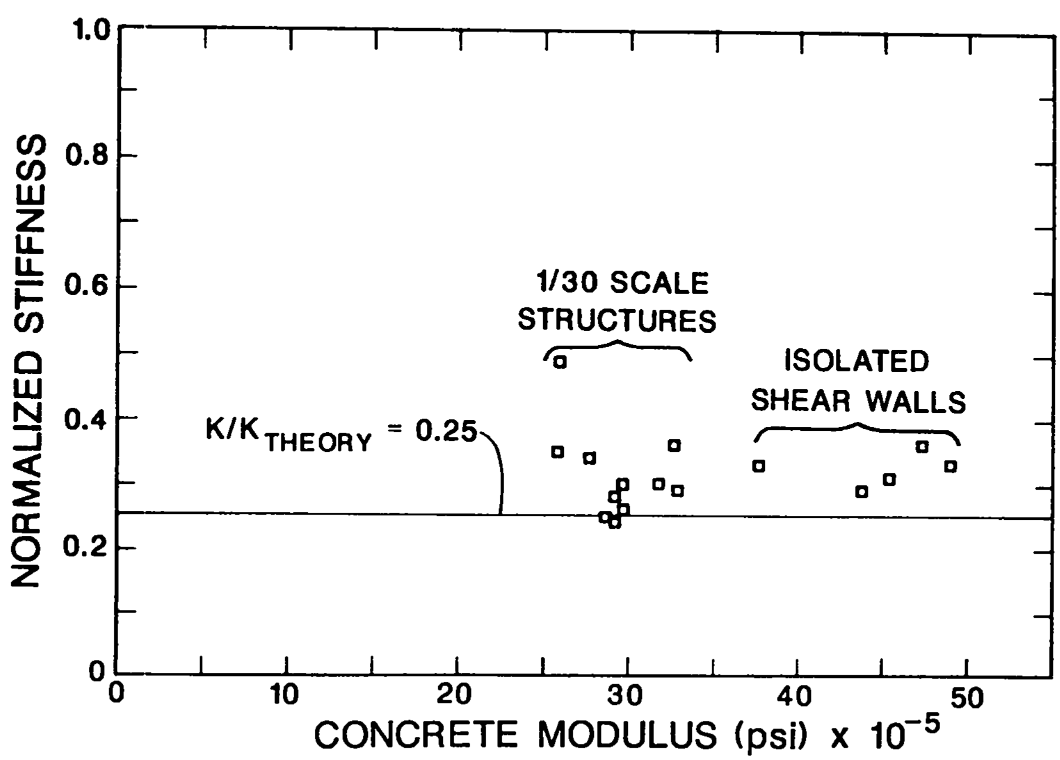

Fig. 7. Normalized stiffnesses vs concrete modulus from this program.

have consistently indicated the same order of reduced stiffness at loads corresponding to 50% of the ultimate load of the structure. However, all tests up to this point in the program were on microconcrete models.

One other possibility for the reduced stiffnesses recorded in these tests was that the connections might be introducing an additional degree-of-freedom that might not be accounted for. For dynamic tests, the question becomes, is shake table motion the same as model base motion?

There are several possibilities for demonstrating that table motion is essentially model base motion. One method is to plot signals from acceleration-time histories taken on the table and on the model base and to visually compare them. Figures 8 and 9 are plots of the table and the model base accelerations over the first portion of a time-scaled earthquake for one of the particular tests. The qualitative comparison of the two records is excellent.

A quantitative comparison can be made in the frequency domain, if we form the transfer function as

$$H(\omega) = \frac{R(\omega)\text{ base acceleration}}{I(\omega)\text{ table acceleration}} .$$

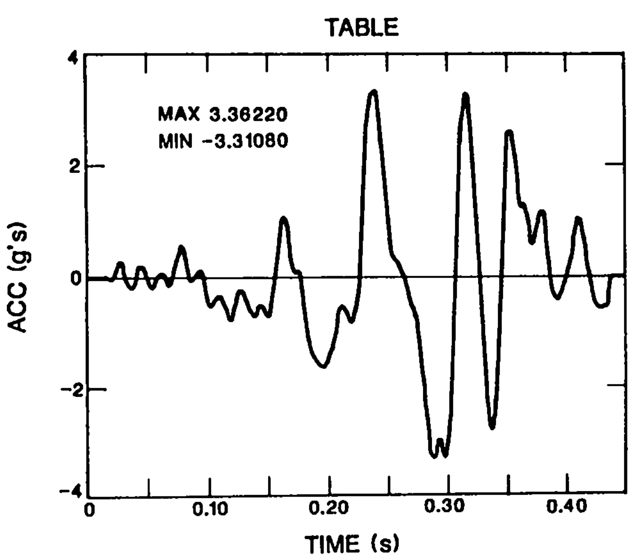

Fig. 8. CERL table acceleration record for CERL Test 1.

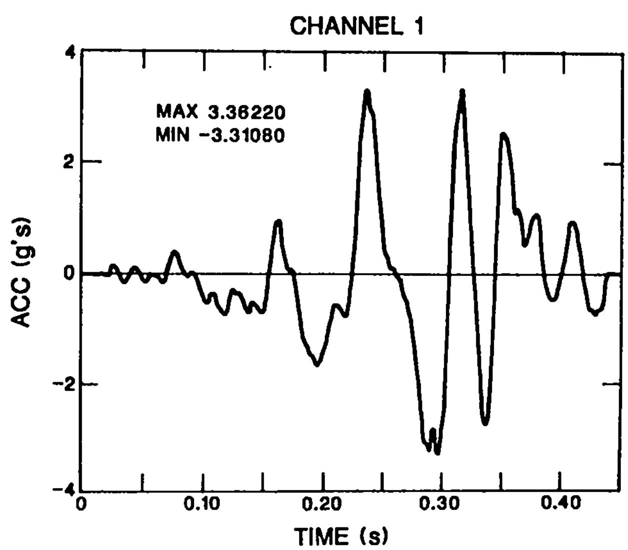

Fig. 9. Model base acceleration record for CERL Test 1.

Then, for identical signals, the following should be true

Real $[H(\omega)] = 1$, and
Im $[H(\omega)] = 0$.

Figure 10 shows the results of this exercise for the records of Figs. 8 and 9. This figure clearly shows that no significant deviation of the two records appears except at some discrete frequencies beyond, say, 75 Hz. To examine the meaning of the "blips," we next turn to the power spectral density (PSD) functions and the cumulative energy integrals. Figure 11 shows the PSD function of the table acceleration, and Fig. 12 shows the PSD function of the model base accelerometer signal. Figures 13 and 14 show the cumulative energies in the two signals as a function of frequency. Examination of Figs. 13 and 14 show that very little energy is contributed to the amplitudes of either signal above 35 Hz. The same information, of course, is shown in Figs. 11 and 12, i.e., there is no significant frequency content in the signals above

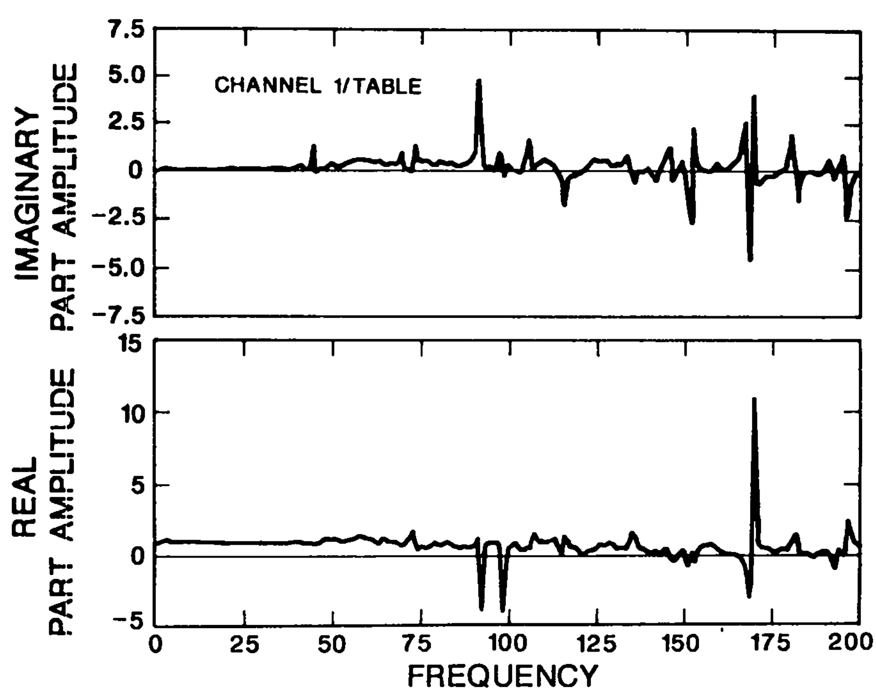

Fig. 10. Imaginary and real parts of the base-to-table acceleration record transfer function.

35 Hz. To quote from Harris and Crede in the section on Measurement of the Transfer Function (Ref. 8, Section 23.30), "Accurate values of H(ω) are obtained only in those frequency ranges where f(t) (the input function) has a significant frequency content." In other words, these signals are the same over the frequency range of interest, and thus there is no flexibility being introduced in the base-to-table connections that will affect the measurement of first-mode frequency.

Upon completion of this review, the design of a structure and its models to satisfy the TRG requirements set forth in Section II was undertaken.

V. DESIGN OF THE TRG STRUCTURE AND MODELS

The initial design of the TRG structure to meet the observations and design criteria of Section II was approached from a strength-of-materials point of view. An estimate of the required added mass indicated that on the order

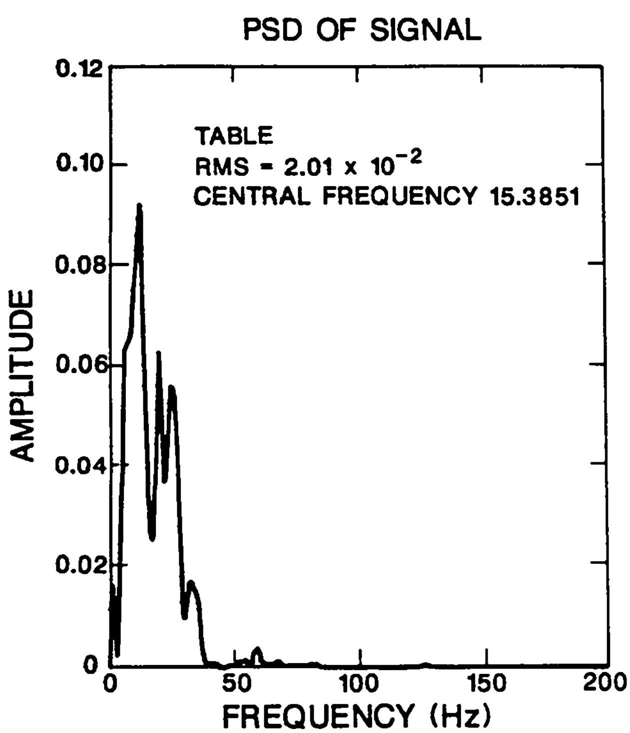

Fig. 11. Acceleration power spectral density for the table accelerometer (i.e., "input" in the transfer function) signal.

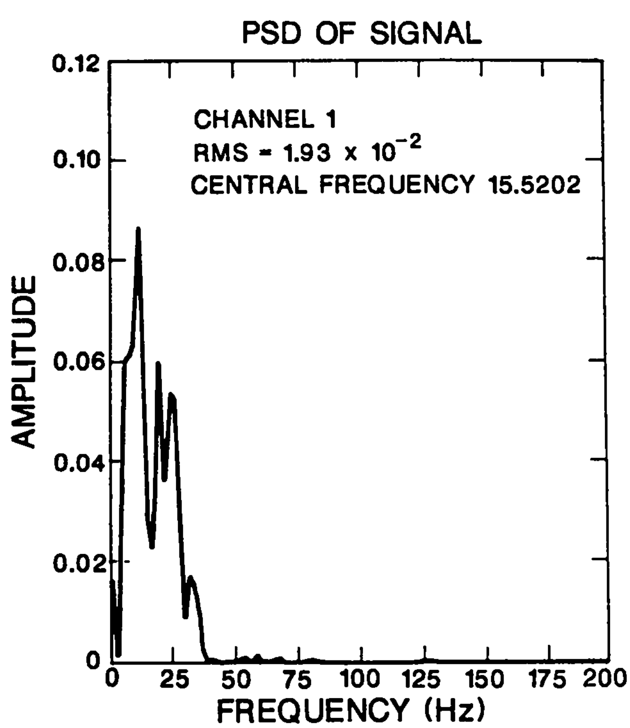

Fig. 12. Acceleration power spectral density for the base accelerometer (i.e., "output" in transfer function) signal.

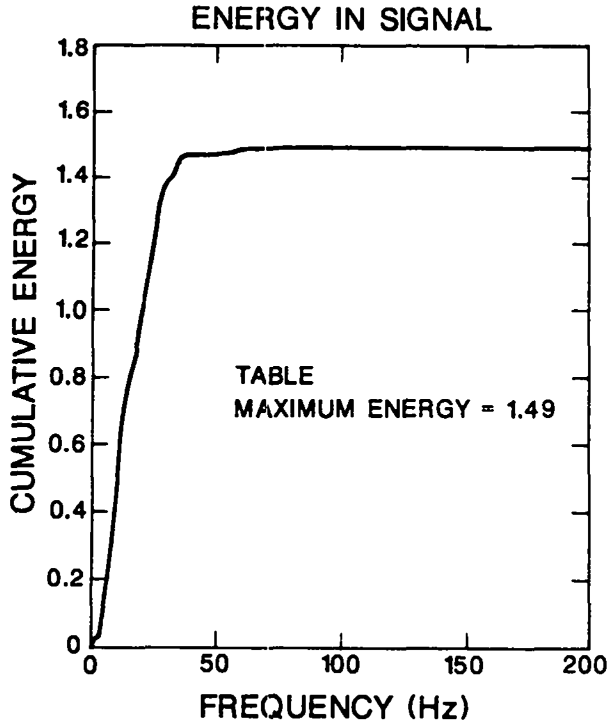

Fig. 13. Cumulative energy integral for the table PSD as a function of frequency.

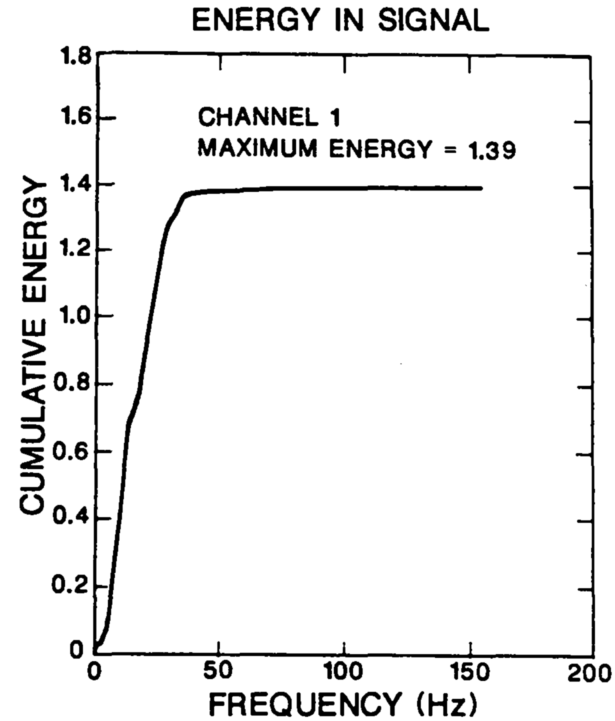

Fig. 14. Cumulative energy integral base accelerometer signal as a function of frequency.

of 3 times the distributed structural mass would be necessary to meet the 30-Hz TRG requirement. It was judged that the effect of such a large added mass should be taken into account in arriving at the force-displacement relationship. Using the free-body diagram of Fig. 15 and making the usual assumptions regarding bending, transformed sections, and effective shear area, an expression for the strain energy for the structure can be written down. Assuming an elastic system, Castigliano's 2nd theorem can be applied to the expression to show that the shear force (V) vs transverse displacement (δ) relationship is

$$\delta = V \left(\frac{hL^2}{2EI_t} + \frac{L^3}{3EI_t} + \frac{L}{A_e G} \right) , \qquad (1)$$

where

E = Young's modulus for concrete,

I_t = transformed section moment of inertia,

A_e = transformed section effective shear area,

G = shear modulus for concrete,

and the geometric parameters L, h are defined in Fig. 15.

The stiffness quantities are defined as

$$K_{CB} = K_{\text{cantilever bending}} = \frac{3EI_t}{L^3} ,$$

$$K_S = K_{\text{shear}} = \frac{A_e G}{L} , \text{ and}$$

$$K_{BM} = K_{\text{bending moment}} = \frac{2EI_t}{hL^2} .$$

The expression for the total stiffness (K_T) then becomes:

$$\delta = V\left(\frac{1}{K_T}\right) = V\left(\frac{1}{K_{BM}} + \frac{1}{K_{CB}} + \frac{1}{K_S}\right) .$$

A simple expression for the first-mode structural frequency (f) for the bending and shear response then becomes

$$\omega = 2\pi f = \sqrt{\frac{K_T}{M_A + M_D}} \tag{2}$$

where,

M_A = the added mass, and

M_D = the distributed mass of the structure.

The expression for the added weight required for a targeted frequency can then be approximated as:

$$W_A = 386 \frac{K_T}{4\pi^2 f^2} - \frac{33}{140} M_{\text{concrete}} , \tag{3}$$

where,

W_A = added weight in lb,

K_T = total stiffness in lb/in.,

f = targeted natural frequency in Hz, and

M_{concrete} = total structural mass of concrete in lb-s^2/in.

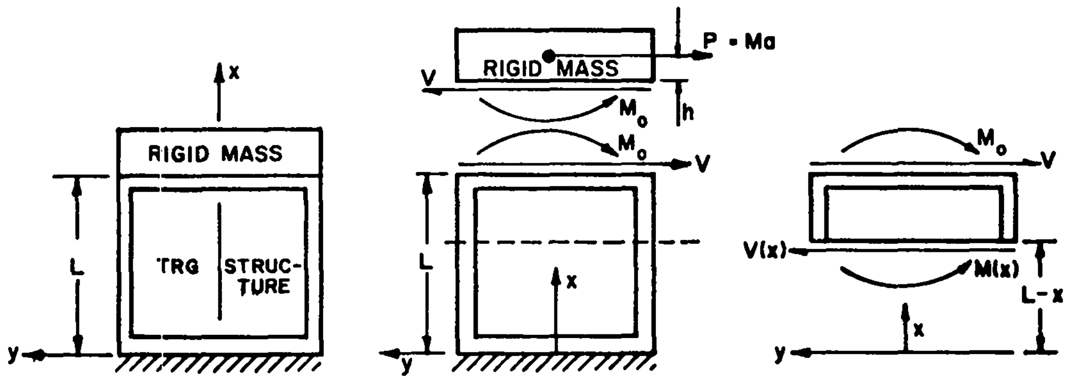

Fig. 15. Free-body diagrams for TRG structure.

The factor 33/140 is from a "Rayleigh's Method" analysis* of a cantilever beam and is used to estimate the effective structural mass of the concrete.

Using these equations and considering the other requirements of the TRG, the structure in Fig. 16 was proposed and approved by the TRG as being acceptable. The characteristics of this structure are given in Table III.

VI. A 1/4-SCALE TRG STRUCTURE

Treating the TRG structure of Fig. 16 as the "prototype," the decision was made to first construct 1/4-scale Case-I type models from microconcrete. A complete discussion of scaling laws for concrete seismic models is given in Ref. 6. Briefly, in a Case I model, the mass is scaled by the length scale cubed. All gravitational effects are distorted (too low) by a factor of the length scale. For example, normal dead weight stresses are 10 psi instead of 40 psi in a 1/4-scale model, but both values are small compared with the cracking strength of the concrete. Overturning moment due to gravity is low by 4, but the overturning moment due to the inertia force is scaled correctly, and

*See example 1.5-3, page 19 of Ref. 9.

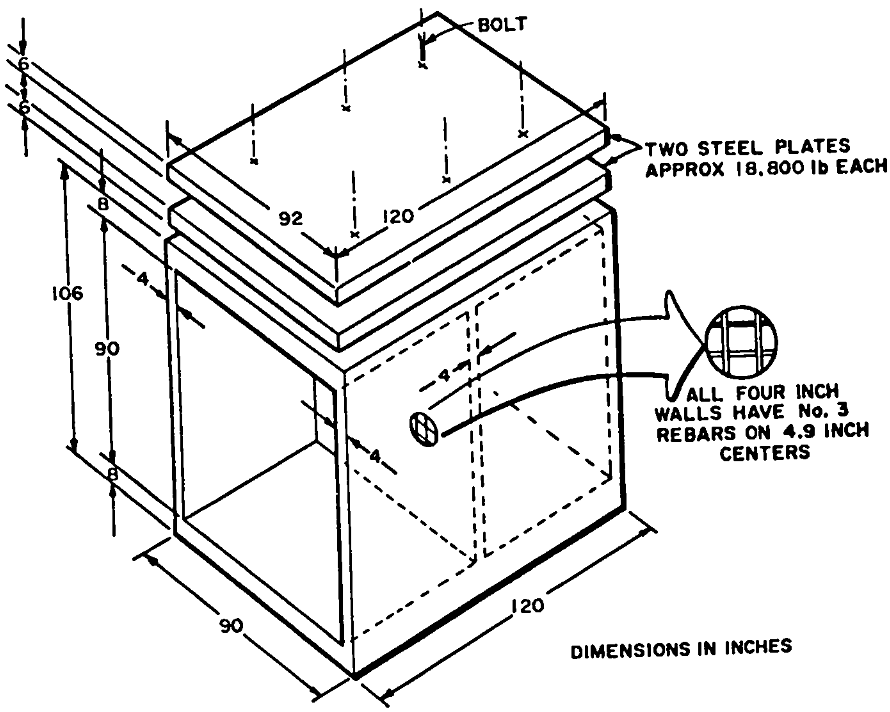

Fig 16. Structure proposed to meet the TRG requirements (hence, "TRG structure").

TABLE III

COMPUTED CHARACTERISTICS OF THE TRG STRUCTURE

Wall thickness	= 4 in.
$I_{\text{uncracked transformed section including steel}}$	= 2.06×10^6 in.^{4}
A-effective shear area	= 379 in.^{2}
Area total (plan view)	= 1288 in.^{2}
Total uncracked bending stiffness	= 2.5×10^7 lb/in.
Shear stiffness	= 5.3×10^6 lb/in.
Total stiffness	= 4.2×10^6 lb/in.
Maximum dead weight normal stress	= 42 psi
Maximum shear stress in flange at 5g due to assumed 5% torsion (approx.)	= 35 psi
Total concrete	= 6 cubic yards
Total added weight	= 37,000 lb
Total weight	= 61,000 lb

is usually orders of magnitude larger than that due to gravity alone. In general, for this model, as with the other models used in this program, the magnitude of the distortions and their effects are understood and are deemed to be acceptable. The major exception is the scaling effects associated with the use of microconcrete.

The purpose of the 1/4-scale models was as follows. First, by applying the same principles of analysis and design and construction practices applied in the previous work, the scalability of the results to the prototype TRG structure could be demonstrated. Second, conclusions (based on calculations) concerning the model and prototype torsional response, individual wall frequencies, out-of-plane bending, and other features that affect the response of the large TRG structure can be confirmed on a less expensive test structure. Third, instrumentation and other data acquisition requirements could be worked out in advance of the larger-scale tests.

A. Construction of 1/4-Scale Model

The model was constructed of microconcrete. A double row of 1/4-inch hail screen reinforcing simulating 0.56% steel in each direction was placed on the centerline of each end wall and the shear wall. The top and bottom slabs were heavily reinforced with No. 3 bars. Figure 17 shows the reinforcing during construction. Properties of the model's reinforcing and the microconcrete are given in Table IV.

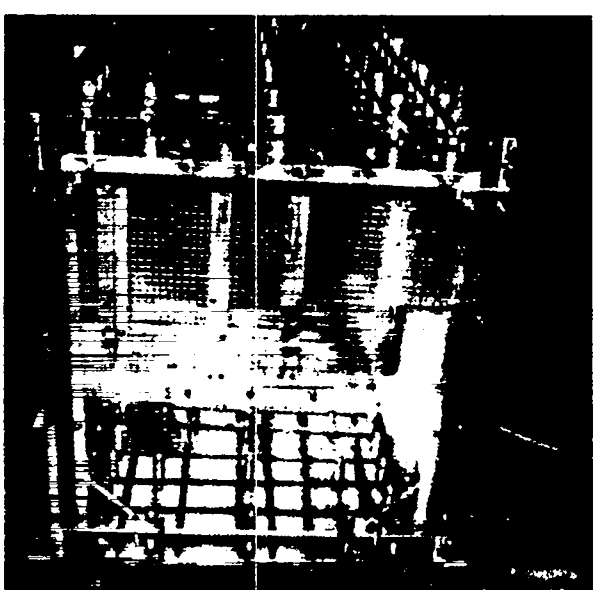

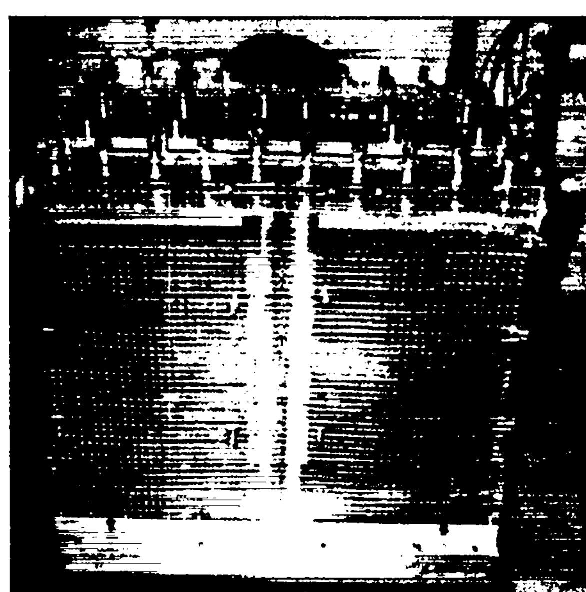

Fig. 17. TRG model (1/4-scale) during construction showing the reinforcing.

TABLE IV

MATERIAL PROPERTIES FOR THE 1/4-SCALE TRG MODEL I

Concrete

E_c	=	(measured at σ-ε origin) = 3.18×10^6 psi
f_c	=	(compressive strength) = 3769 psi
f_t	=	(split tensile test strength) = 513 psi
E_c	=	$57000 \sqrt{f'_c} = 3.5 \times 10^6$ psi

Steel - Bilinear Properties - 0.6% Both Directions

E	=	25.6×10^6 psi
Yield Strength	=	42.7 KSI
Ultimate Strength	=	53.1 KSI
Elongation at failure	=	4%
Diameter	=	0.042 in.

B. Testing Program for the 1/4-Scale TRG Structure

The testing program for this model consisted of a series of very low load-level modal (vibration) and static tests to establish the initial (undamaged) stiffness. These tests were followed by increasingly severe random and simulated seismic testing to failure. The low load-level tests were all "bare" model tests (no added mass) and the random and seismic tests were conducted with 575 lb of added weight. This weight is approximate for a 1/4-scale Case I model of the large 30-Hz TRG structure. A summary of the testing sequence is given in Table V with a more detailed description provided below. Comparison with the analysis will follow the testing results.

1. Low-Level Modal Tests (Free-Free Boundary Conditions). These tests were performed using a 50-lb (maximum) portable shaker suspended from surgical tubing, which excited the structure with a random signal at a preselected point in the direction parallel to the shear wall. The portable shaker was programmed with a signal having a spectral density amplitude rolloff with frequency at about 500 Hz, so that, in general, all natural modes below 500 Hz were strongly excited. Response acceleration was taken in 3 directions at 31

TABLE V

TEST SEQUENCE AND CONDITIONS FOR TRG-1

Test No.	Test Type	Boundary Condition	Added Mass
1	Low-level modal	Free-free	None
2	Low-level static	Fixed-free	None
3	Low-level modal	Free-free	None
4	Low-level modal	Fixed-free	None
5	Random base	Fixed-free	None
6	Random base	Fixed-free	Yes
7	Seismic	Fixed-free	None
8	Seismic	Fixed-free	Yes

points, which provided 93 separate pieces of data. Figure 18 shows a schematic of the structure and the points at which data were taken. The structure was excited at Point 2 parallel to the shear wall. Figure 19 is a photograph of the test setup. The structure was supported on a foam rubber pad to approximate a free-free boundary condition. The response acceleration data were used to construct a matrix of transfer functions that can then be used in several ways to develop the natural modes and resonant frequencies of the structure.

For cases in which modal coupling is small (modal frequencies significantly separated), the response can be treated as a single degree-of-freedom in the vicinity of each modal resonance (see Ref. 10). Software (part of the modal analysis system), for these single degree-of-freedom curve-fitting methods was used on the data to identify the mode shapes and frequencies. The lowest nonrigid body mode for this structure in the free-free condition as a bare model is the torsional mode, which was measured at 112.5 Hz, and the combined bending and shear mode is the second mode, which was measured at 307.5 Hz. It should be noted that the model is designed such that, in the fixed-free condition (with the base of the model fixed against translation and rotation) and with added mass, the bending/shear mode is the lowest mode for this structure.

2. Low-Level Static Tests (Fixed-Free Boundary Conditions). The second series of tests consisted of a series of low-load level static tests. A maximum load level (1380 lb) was calculated that would not allow the predicted

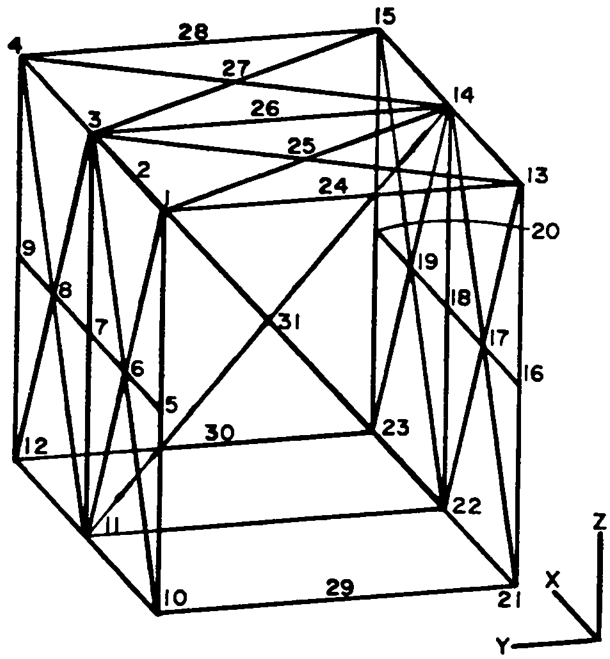

Fig. 18. Schematic representation by modal analysis software of TRG 1-in.-wall model showing 31 points at which data are collected. Point 2 is the load application point.

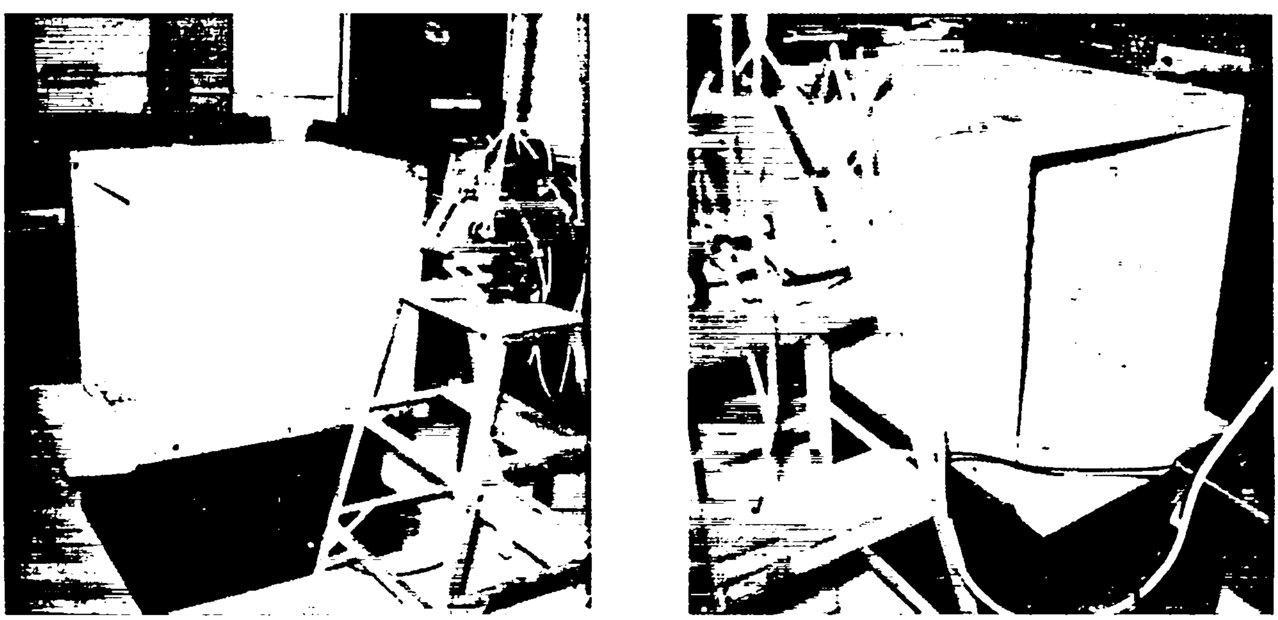

Fig. 19. Photograph of modal testing.

maximum principal stress in the concrete shear wall to exceed 80 psi, which the TRG identified as the maximum stress that would not cause damage to the concrete. The test setup is shown schematically in Fig. 20 and a photograph of the test setup is shown in Fig. 21. The data from the dial gages, the non-contact gages, and the average readings were used to determine the relative displacement of the top of the structure relative to the bottom. The data were then plotted to determine the structural stiffness directly, as shown in Figs. 22-24. Although the noncontact gages were attached to the load frame, indicated relative displacements of the shear wall were about the same values as those of the dial gage. The data seem to show that the loading frame is relatively stiff compared with the structure, and frame deformation would not act to influence the measured stiffness. However, one area of concern for the large test will be to ensure that true relative displacements of the shear wall structure itself are obtained, because it will be difficult to design a loading frame stiffer than the structure itself.

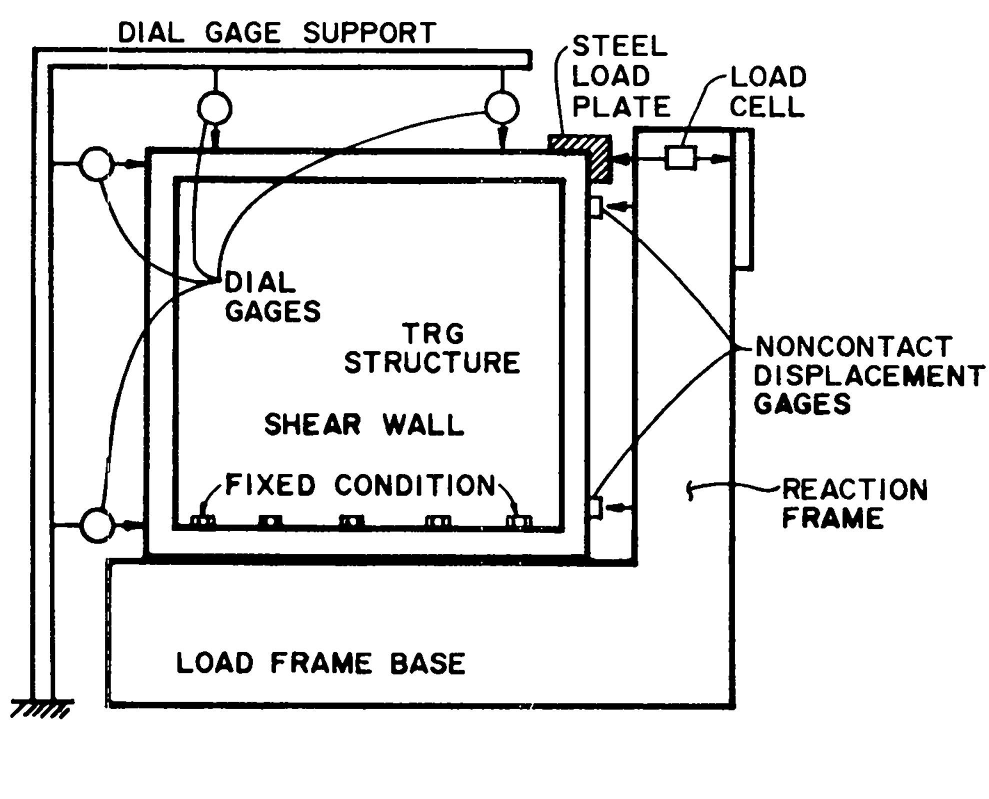

Fig. 20. Schematic of the low-load level static test setup.

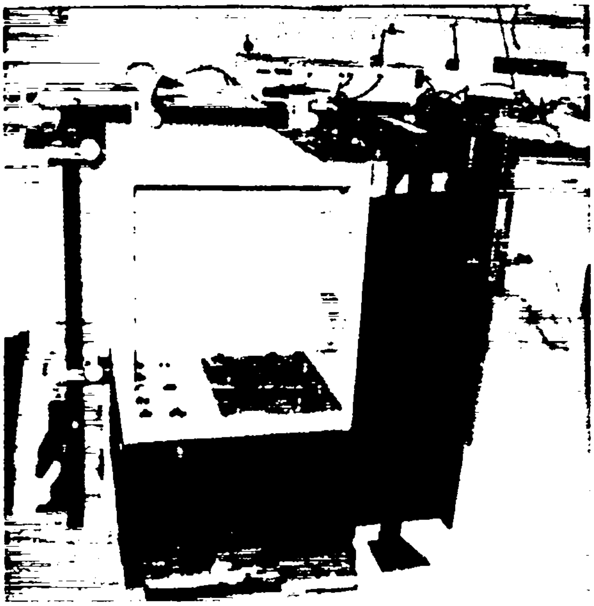

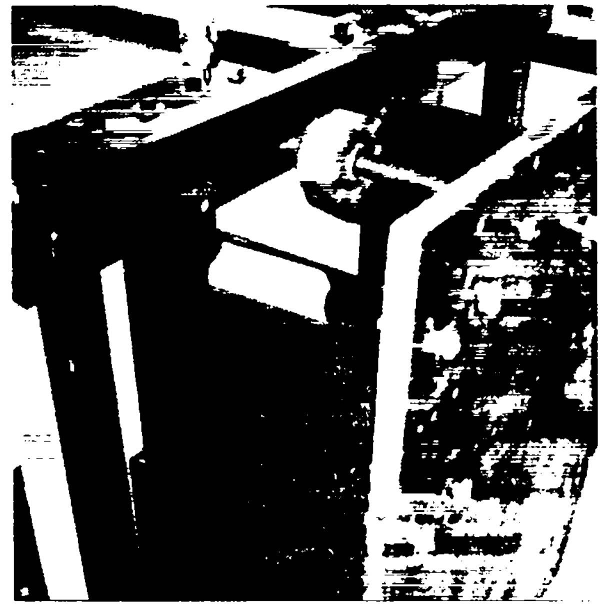

Fig 21. Photograph of low-level static test setup.

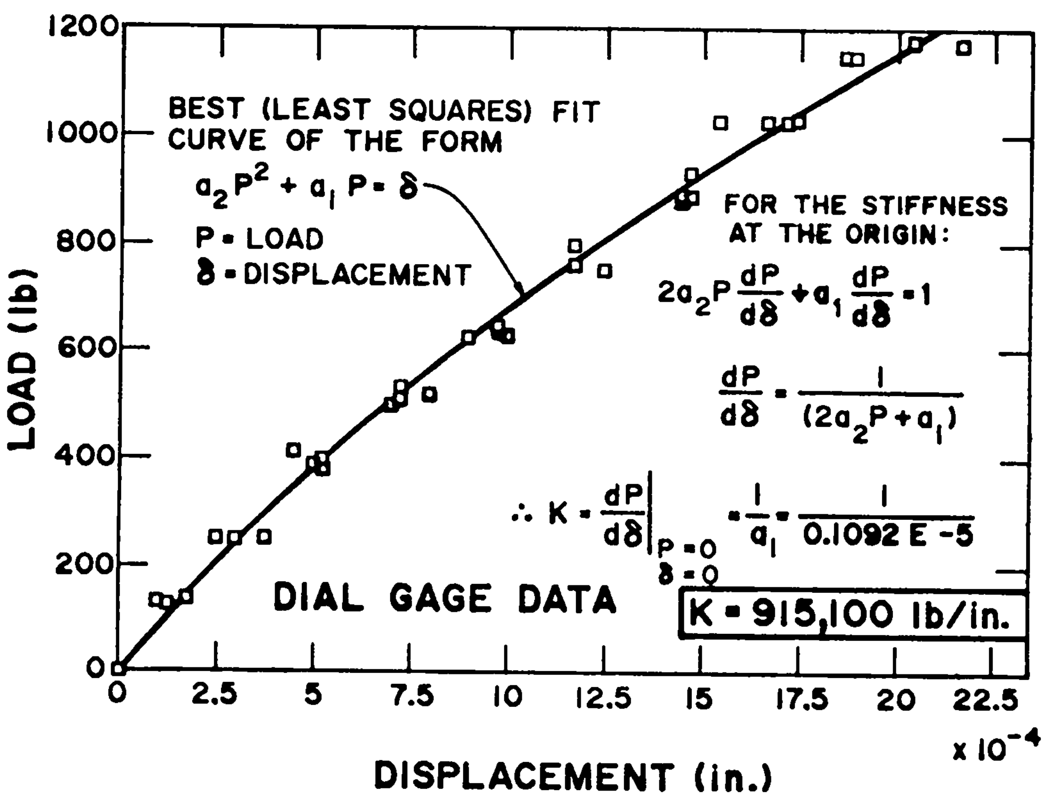

Fig. 22. Plot of load-displacement curve from all dial gage data.

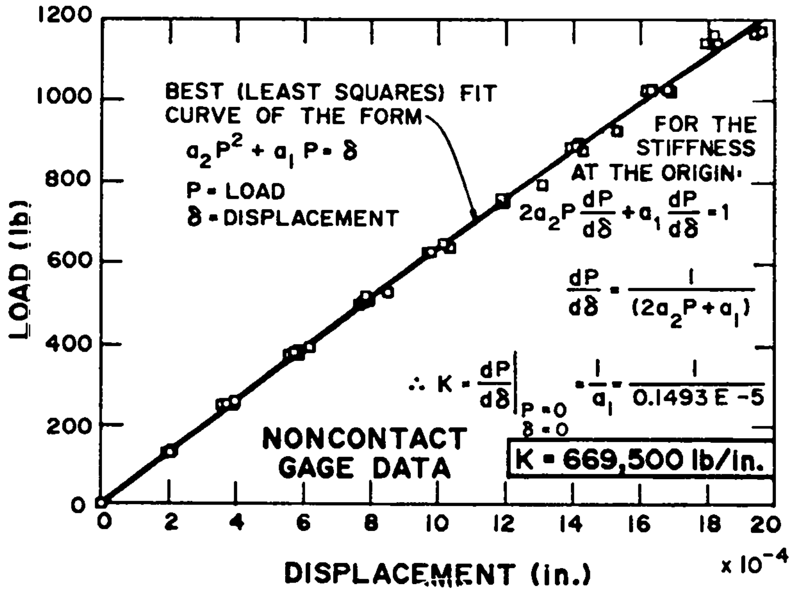

Fig. 23. Plot of load-displacement curve from all noncontact gage data.

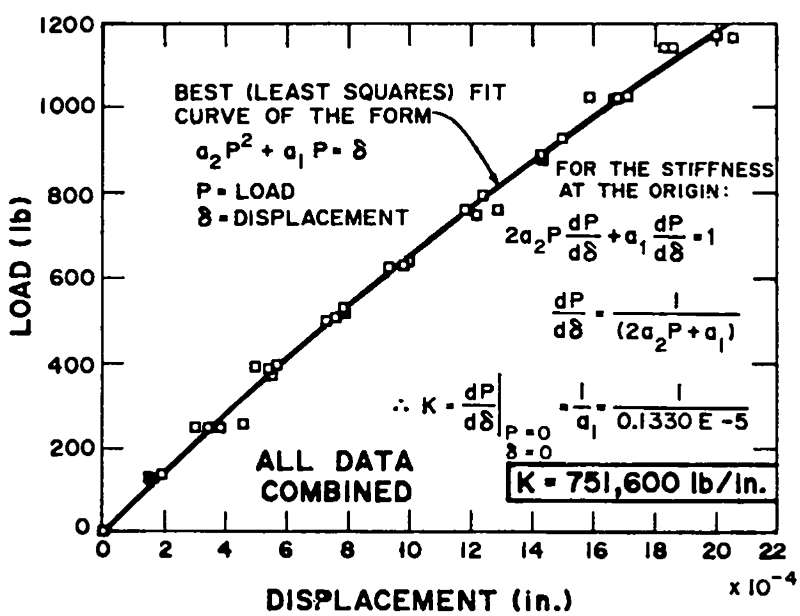

Fig 24. Plot of all static test data combined by averaging the corresponding dial gage and noncontact gage readings for a given test point.

The method used to determine the stiffness at the origin was to perform a least squares fit to the load deflection data using a quadratic expression,

$$a_1P^2 + a_2P = \delta ,$$

where P is the applied load, δ is the relative displacement, and a_1 and b_2 are fitting constants. The stiffness was then determined analytically as the slope at the origin and is equal to $1/a_2$, as shown in Figs. 22-24.

3. Low-Level Modal Test (Free-Free Boundary Conditions) Repeated. Following the low-load level static tests, the model was transported (10 miles) to the Los Alamos electro-dynamic shaker facility. To determine if any significant damage had been done during static testing or during transportation, the modal tests (described in 1 above) were repeated. The torsional mode measured at 107.5 Hz and the shear deformation mode at 293.8 Hz were both down by 4.4% from the values found during initial testing. It is not clear that such a small reduction is indicative of damage or variation in test conditions. However, we did make the following observation. After the static test phase, a visible crack appeared part way through the bottom slab. The crack did not extend to the shear wall, and it had not been observed in the model before static testing. There were no other observable cracks nor did any of the pretest shrinkage cracks appear to extend or change in any manner. It is easy to believe that a 4.4% reduction in frequency would be indicative of this damage, but more experience in modal testing of concrete structures must be acquired on our part to have confidence in this degree of accuracy.

4. Low-Level Modal Testing (Fixed-Free Boundary Condition). After mounting the model on the shaker table, the modal testing was repeated again using the random excitation at Point 2 (see Fig. 18). With the shake table locked in position, the base fixity can be checked by noting that the relationship between the free-free frequencies and the fixed-free frequencies for the bending/shear deformation mode is

$$\overset{\text{free}}{f^{\text{free}}} = \sqrt{2}\, \overset{\text{fixed}}{f^{\text{free}}} \quad .$$

If we use the value $f^{free-free}$ = 307.5 Hz, measured above in Test 1, the implied fixed-free condition frequency would be 217.25 Hz. The measured frequency was 221.25 Hz, less than a 2% difference. This test result confirms that the fixed base condition for the model is adequate for the shear/bending mode of interest. A further comment is in order about why we chose to use f = 307.5 Hz as the free-free condition of comparison, rather than f = 293.8 Hz, as measured in Test Series 3. Using the value of f = 293.8 Hz as the free-free frequency would give 207.75 Hz as the fixed-free frequency, a difference of 6.5% (a value that may still be within experimental error for these tests). The justification for the choice of 307.5 is that, if the decreased value (307.5 from Test 1 to 293.8 Hz from Test 3) is indeed indicative of the damage noted by inspection of the cracked model following the static testing, then this damage occurred in the base slab that is now part of the "fixed" boundary. Then, because no damage was apparent in the rest of the model, there should not be a reduction in the fixed-free frequency. The data appear to bear this conclusion out; but again, more experience in modal testing of reinforced concrete structures should be acquired to know if such a claim can be supported.

5. Random Base Motion (1/2-g) Bare Model Test. With the model clamped on the table, the shaker was used to apply a random signal at the model base. The shaker and control system characteristics are such that the signal level must be about 1/2-g input for good control. The measured shear-bending mode frequency was 192.6 Hz (mode shape in Fig. 25). Because this value is down by 13% from the fixed-free Test 4, it is taken as an indication that damage to the model had occurred.

This point is very important and will be addressed again in the discussion of the results. We note here that this test would be indicative of the first dynamic test that would have been run on all of the previous 3-D box-like models.

6. Random Base Motion (1/2g) with 575 lb of Added Weight. Following the random base motion bare model tests, a weight of 575 lb was attached to the top of the model. Random 1/2-g base motion was again applied and the mode shapes and frequencies were determined. The shear-bending mode natural frequency was measured as 76.6 Hz, with the mode shape as shown in Fig. 26. A simple calculation based on Eq. 2, using M_d = 0.415 lb-s^2/in., and f = 192.6 Hz (from Test 5), would indicate that, if no further damage occurred, this frequency should have been 89.8 Hz. This further reduction in natural

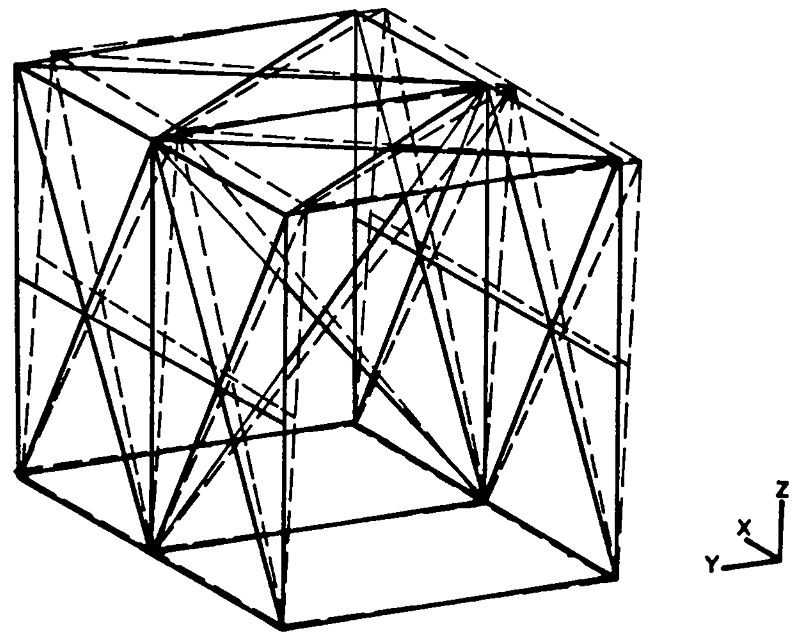

Fig. 25. Bare model shear-bending mode shape determined from modal testing as a fixed-base model.

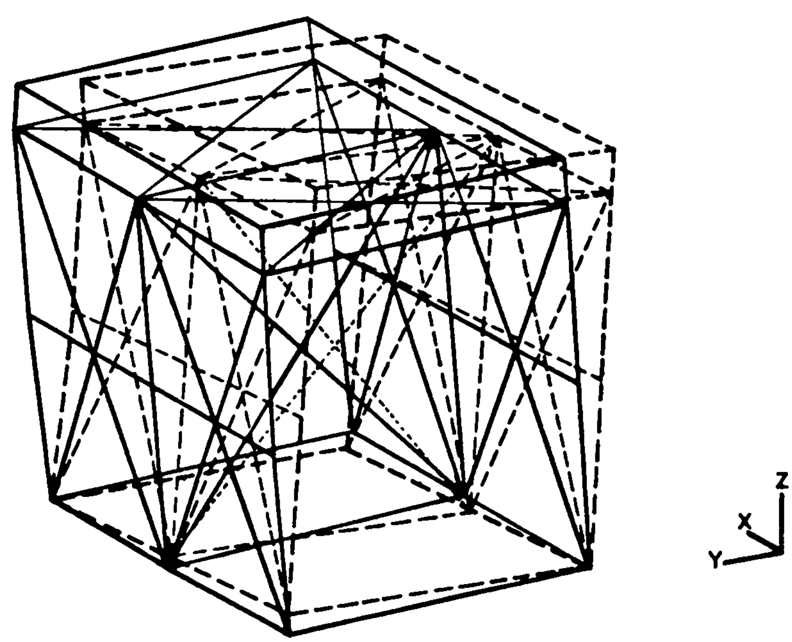

Fig. 26. Shear-bending mode shape from modal testing as a fixed-base model with added mass. (1/4 scale model of a TRG structure).

frequency for this mode was accompanied by visible cracking and crack extension at the top-slab corner interface and at the base of the shear wall.

The significant point about this test is that the derived stiffness based on this "low" load level is indicative of the initial stiffnesses that would have been reported in all of our previous 3-D model tests.

The amplification factor for this test was about 1.8. Thus, the average base shear stress can be computed from beam theory to be about 30 psi for this 1/2-g nominal test. The bending stress (assuming a fully effective end wall) at the wing wall and shear wall intersection is about 20 psi. The resultant maximum principal stress, neglecting the normal stress due to the added mass, is about 40 psi. Because this value is well below the tensile strength of the material (513 psi), reduced stiffness due to cracking would not normally be expected. Speculation about the actual cause of the reduced stiffness centers about cracking. However, it may be that coalesing shrinkage cracks and cyclic loading has a large effect in these small models.

7. Bare Model Seismic Tests. Following these two basic tests, a test plan was carried out that is similar or identical to all previous 3-D model tests. The top mass was again removed from the model and a series of 1/2-g seismic random signals was used to drive the model. Table VI shows this set of bare model tests, in the order applied and the natural frequency results.

The "low-level" (1/2-g) random signal is used as a tickle test to indicate changes in natural frequency following each seismic test. As can be seen from Table VI, no further damage was indicated up through 1.3 g.

TABLE VI

BARE MODEL SEISMIC TESTS

Test No. and Type	Peak Accelerations Positive g	Peak Accelerations Negative g	Indicated Shear-Bending Mode Natural Frequency
1. L.L. Random	0.5	-0.5	186.9
2. Seismic	0.5287	-0.3747	-
3. L.L. Random	0.5	-0.5	186.9
4. Seismic	0.6530	-0.4945	-
5. L.L. Random	0.5	-0.5	186.9
6. Seismic	1.004	-0.7024	-
7. L.L. Random	0.5	-0.5	186.9
8. Seismic	1.315	-0.911	-

8. Seismic Test as a TRG Structure 1/4-Scale Model. The 575 lb of additional weight was again added to the structure and a sequence of simulated seismic tests followed by low-level random tests was carried out. The seismic signal was the N-S El Centro Earthquake time-scaled by a factor of 20. This earthquake record has been base-line corrected and was chosen to have a peak acceleration response in real time of about 3 Hz. If we assume the prototype TRG structure represents about a 1/5-scale structure, so that the earthquake that we apply to it will have a peak response of about 15 Hz, then the signal as time-scaled by the factor of 20 is correctly scaled to simulate the corresponding input for a 1/4-scale model of the TRG structure. Under this assumption, accelerations of 1 g on a Category I building would correspond to 5 g on the TRG structure and 20 g on the 1/4-scale model. Table VII shows the test sequence and the results. As the magnitude of the input signal was increased, the structural stiffness degraded. For all practical purposes, the specimen was completely failed at the 8.9-g level. The additional pulse at 14.6-g level separated the hail screen reinforcing in tension on one entire side of the model. The initial failure mode, however, was the sliding shear failure mode seen in our previous test of 3-D model structures. Classical diagonal cracks in the shear wall were present from Test Series No. 6. During this seismic sequence, new ones appeared and former ones extended and widened. Figure 27 shows the failed TRG structure.

C. Finite Element Analysis of 1/4-Scale TRG Model Structure

A finite element idealization of the 1/4-scale TRG model structure was analyzed using the ABAQUS finite element code. ABAQUS is a commercially available code for general purpose structural and thermal analysis. Results obtained from the analysis are compared with both experimentally measured static and dynamic response and with calculations based on a strength-of-materials approach derived in Section V and entitled "Design of the TRG Structure and Model."

The structure was modeled using general shell elements with a rebar option. The rebar option smears the actual reinforcement pattern into a unidirectional membrane of constant thickness. Only a quarter section of the structure was modeled because of symmetry, thus reducing the number of nodes and elements in the model and increasing computational efficiency.

The analysis was broken into two separate procedures. First, the natural frequencies and mode shapes were determined for the six lowest nonrigid body

TABLE VII

SEISMIC TESTING TO FAILURE OF THE 1/4-SCALE TRG STRUCTURE

Test No. and Type	Peak Accelerations Positive g	Peak Accelerations Negative g	Indicated Shear-Bending Mode Natural Frequency Hz
1. L.L. Random	0.5	- 0.5	75.1
2. Seismic	0.499	- 0.366	-
3. L.L. Random	0.5	- 0.5	76.1
4. Seismic	0.968	- 0.7925	-
5. L.L. Random	0.5	- 0.5	75.1
6. Seismic	1.92	- 1.56 4	-
7. L.L. Random	0.5	- 0.5	75.1
8. Seismic	4.17	- 3.59	-
9. L.L. Random	0.5	- 0.5	68.7
10. Seismic	4.86	- 4.57	-
11. L.L. Random	0.5	- 0.5	61.8
12. Seismic	8.88	- 7.98	-
13. L.L. Random	0.5	- 0.5	45.0
14. Seismic	0.87	- 0.82	-
15. L.L. Random	0.5	- 0.5	41.2
16. Seismic	14.65	-17.77	-

modes. Second, a static load deflection curve was obtained in the elastic range. To develop a static load-deflection curve, the nodes representing the bottom plate of the structure were completely constrained to simulate the fixed-base condition that we assume the bolts in the actual structure provide. In the dynamic analyses, appropriate boundary conditions (i.e., asymmetric conditions along both axes of symmetry for torsional response, etc.) were applied along the axes of symmetry to obtain the desired mode. Because modal testing was done with free-free end conditions, these conditions were also reproduced in the finite element modal analysis.

The first computations were completed prior to the determination of actual concrete properties for the test structure. Hence, elastic material properties were estimated for both concrete and reinforcement. Subsequent runs were made with material properties adjusted to bring natural frequencies and stiffness in line with experimental values, and, finally, runs were made with material properties measured from actual test specimens.

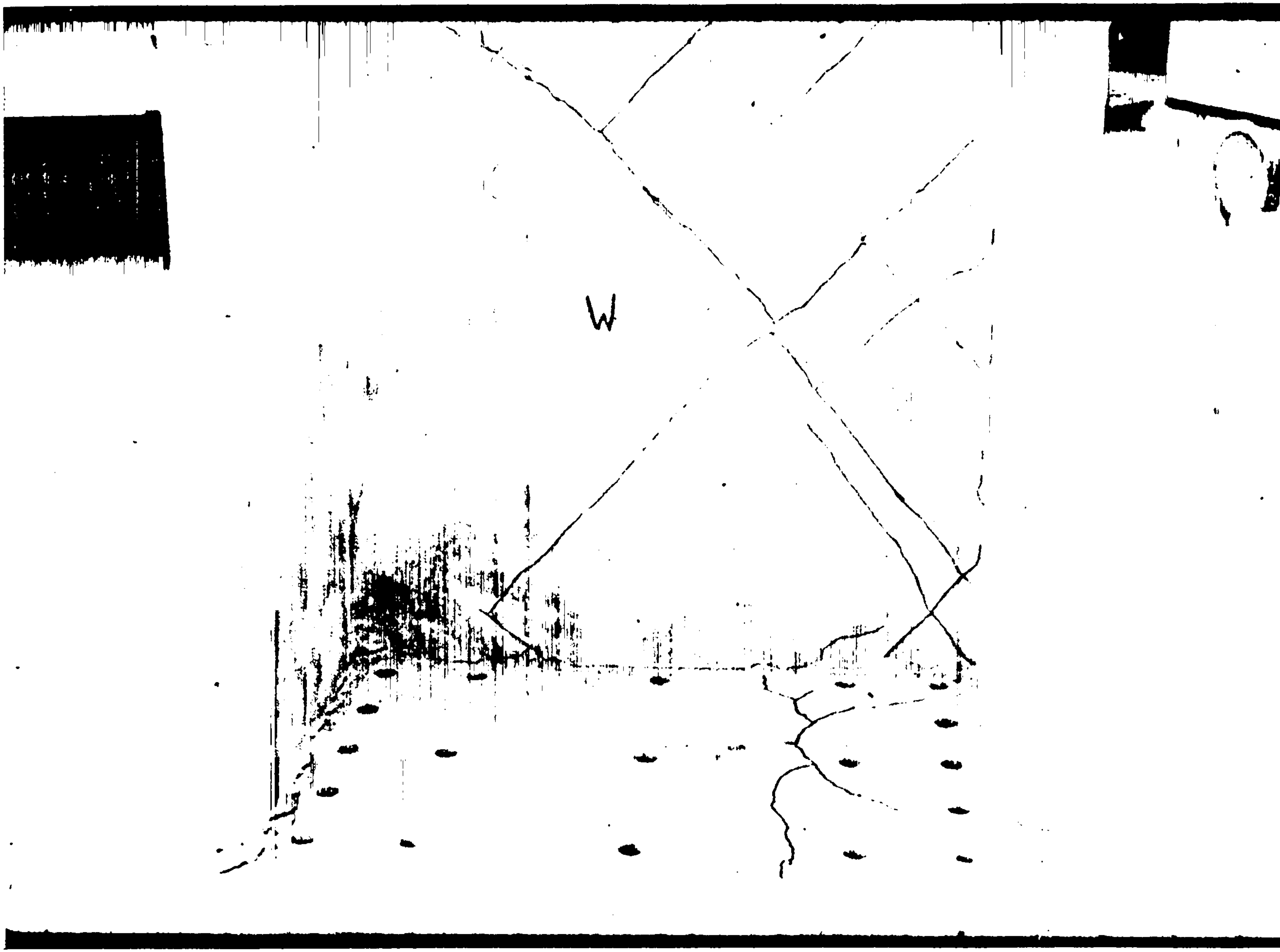

Fig. 27. Photograph of the failed model.

Initial results using estimated material properties yielded natural frequencies approximately 10% below those measured during low-level modal testing. Because frequency is related to the square root of elastic modulus, a second run was made with the modulus increased (by 21%)[2]. Results of that run were almost identical to the low-level modal analysis results.

D. Determination of Initial Stiffness of the 1/4-Scale TRG Structure

The primary purpose of all low-level tests was to compare the so-called "undamaged" stiffness or virgin model stiffness with the theoretical values. A model shear-bending stiffness was deduced from all modal and low-level static tests and these values are given in Table VIII. The consistency of the values between static (direct measurement) and dynamic (indirect measurement) methods is good for the initial stiffness test results.

Table IX presents the results of all calculated values, using both the strength-of-materials approach and the finite element model and the three various estimates for the concrete modulus, $E_c = 3 \times 10^6$ psi (design value), $E_c = 3.18 \times 10^6$ psi (strain gage measured value), and $E_c = 3.5 \times 10^6$ psi (ACI Method, $E_c = 57000\sqrt{f'_c}$).

TABLE VIII

MEASURED VALUES OF INITIAL STIFFNESS

	Stiffness $\times 10^6$ lb/in.
Static or Direct Measurements (Figs. 22-24)	
1. Dial gauge data (Fig. 22)	0.915
2. Noncontact gauge data (Fig. 23)	0.695
3. Combined readings for static data (Fig. 24)	0.752
Dynamic or Indirect Measurements (Based on Eq. 2)	
4. Free-free modal Test Series 1	0.775
5. Free-free modal Test Series 3	0.707
6. Fixed-free modal Test Series 4	0.802
Average value from all data, 1-6	0.774

TABLE IX

CALCULATED VALUES OF STIFFNESS

Method and Assumptions	$\times 10^6$ lb/in.
Strength-of-materials approach	
1. $E_c = 3 \times 10^6$ psi	1.09
2. $E_c = 3.18 \times 10^6$ psi	1.15
3. $E_c = 3.50 \times 10^6$ psi	1.27
Finite element method	
4. $E_c = 3 \times 10^6$ psi	0.860
5. $E_c = 3.18 \times 10^6$ psi	0.910
6. $E_c = 3.50 \times 10^6$ psi	1.00

E. Discussion of Results of the 1/4-Scale TRG Structure Tests

Two points are clear regarding the measured initial stiffness of the model and the so-called "working-load" stiffness. First, from Tables VIII and IX, it can be shown that the initial stiffness that is measured is about 70-80% of the theoretical value. This 20 - 30% reduction in stiffness is probably caused by shrinkage cracking and other imperfections associated with fabrication of concrete models. Comparison of this model with identical fabricated models can indicate the magnitude of such variations. However, the second point is that there was a definite change in stiffness characteristics of this structure when a significant dynamic load was applied. This point is clearly indicated in the test series in which the natural frequency as a fixed-base model deteriorated from 221.25 Hz in Test Series 4 to 192.6 Hz in Test Series 5. This 13% decrease in natural frequency corresponds to a 24% decrease in structural stiffness and is a clear indication of the occurrence of structural damage during the 0.5-g random base motion applied in Test 5. Furthermore, the model suffered even more damage during Test Series 6. The frequency decreased 14%, corresponding to an additional 25% decrease in stiffness. The measured value of 76.6 Hz in Test Series 6 implies a stiffness of 441,220 lb/in., approximately 38% of the value that would be calculated by an uncracked strength-of-materials approach. This value is consistent with values reported in all of our previous tests on the 3-D structures. Figure 28 illustrates this point that shows the normalized measured stiffness, reported from previous tests and this current model test structure, when it was subjected to the same testing procedure as the previous tests on the 3-D test structures.

The bothersome point about this result is that the stress levels in the dynamic test that can be calculated (40 psi) are not large enough to indicate significant damage from additional cracking, yet all indications (decreased first mode frequency and visual inspection of model corners) point to this being the case. The actual mechanism for reduced stiffness is still poorly understood.

VII. CONCLUSION AND RECOMMENDATIONS AT THE END OF FY 1985

There have been no surprises so far from the testing of this first TRG model structure. The model behaved in the manner expected and the data appear to be consistent with our previous data on 3-D test structures. The data also

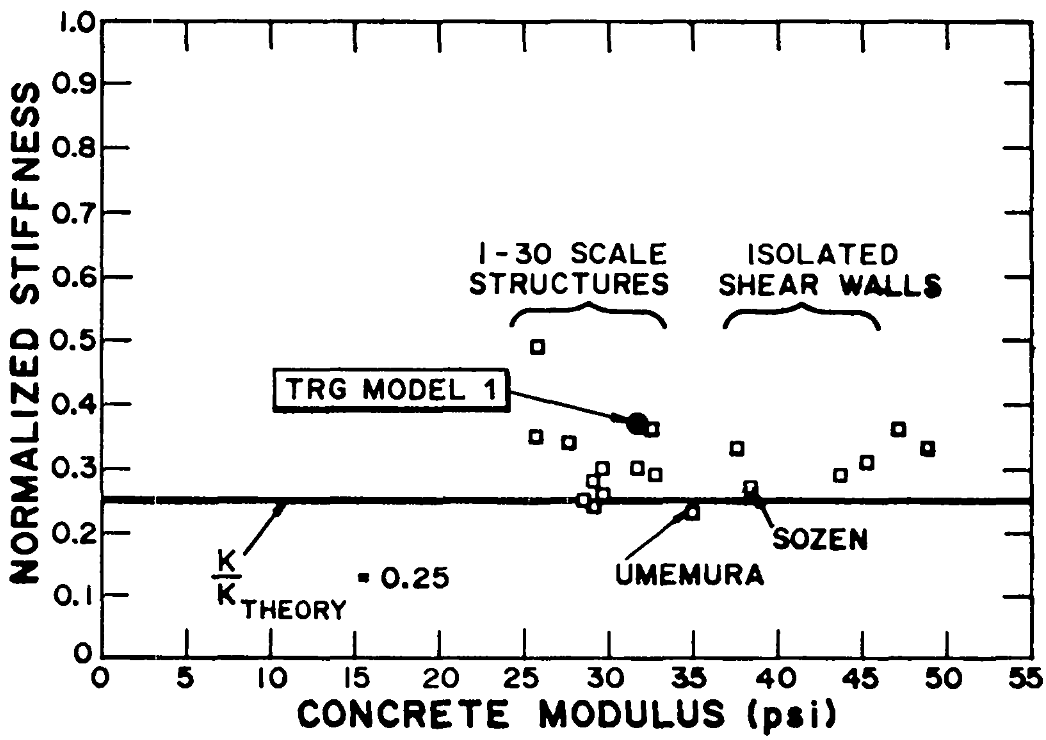

Fig. 28. Normalized stiffnesses vs concrete modulus from this program and others, showing the 1/4-scale TRG model after being subjected to 1/2-g seismic test.

support our contentions that stiffnesses at "working loads" can be significantly lower than usual industry practice assumes. However, the effect of microconcrete and the reproducibility of the results must still be investigated.

Several weaknesses in our current test and fabrication procedures were revealed and will be corrected. For example, we will go to the standard ASTM cylinder and to measure concrete properties, rather than use model ASTM cylinders.

On the other hand, some new test procedures used here were encouraging. The low-level modal tests gave data consistent with our static data. Modal testing of reinforced concrete structures is at the state-of-art of this testing technology; that is, it has not been widely used for reinforced concrete.

The current recommendation is to continue with the TRG series test models and structures. (The first large TRG prototype was under construction at the end of FY 1985.) The geometry appears to be adequate, the response is predictable from calculations, and the data are consistent between tests.

REFERENCES

1. E. G. Endebrock, R. C. Dove, C. A. Anderson, "Margins to Failure - Category I Structures Program: Background and Experimental Plan," Los Alamos National Laboratory report NUREG/CR-2347 (December 1981).

2. E. G. Endebrock, R. C. Dove and C. A. Anderson, "Seismic Category I Structures Program," Proceedings of the 12th Water Reactor Safety Information Meeting, National Bureau of Standards, October 22, 1984, Bethesda, Maryland.

3. R. C. Dove, E. G. Endebrock, W. E. Dunwoody, and J. G. Bennett, "Seismic Tests on Models of Reinforced Concrete Category I Buildings," 8th International Conference on Structural Mechanics in Reactor Technology, Brussels, Belgium, August 19-23, 1985.

4. E. G. Endebrock, R. C. Dove, and W. E. Dunwoody, "Analysis and Tests on Small Scale Shear Walls - FY 82 Final Report," Los Alamos National Laboratory report NUREG/CR-4274 (September 1985).

5. R. C. Dove, J. G. Bennett, C. R. Farrar, and C. A. Anderson, "Seismic Category I Structures Program Final Report, FY 1983-84," Los Alamos National Laboratory report, LA-11013-MS, NUREG/CR-4924 (July 1987).

6. R. C. Dove and J. G. Bennett, "Scale Modeling of Reinforced Concrete Category I Structures Subjected to Dynamic Loading," Los Alamos National Laboratory report NUREG/CR-4474 (January 1986).

7. J. G. Bennett, R. C. Dove, W. E. Dunwoody, E. G. Endebrock, C. R. Farrar, and P. Goldman, "Simulated Seismic Tests on 1/42 and 1/14 Scale Category I Auxiliary Buildings," Los Alamos National Laboratory report LA-11093-MS, NUREG/CR-4987, (August 1987).

8. C. M. Harris and C. E. Crede, Eds., Shock and Vibration Handbook, 2nd ed. (McGraw Hill Book Company, New York, 1976).

9. W. T. Thompson, Vibration Theory and Applications (Prentice-Hall, Englewood Cliffs, New Jersey, May 1965).

10. D. J. Ewins, Modal Testing (John Wiley and Sons, Research Studies Press Ltd., Letchworth, Hertfordshire, England, June 1985).

DISTRIBUTION

	Copies
Nuclear Regulatory Commission, RA, Laurel, Maryland	248
Technical Information Center, Oak Ridge, Tennessee	2
Los Alamos National Laboratory, Los Alamos, New Mexico	50
	300

NRC FORM 336 (2-84) NRCM 1102, 3201, 3202

U.S. NUCLEAR REGULATORY COMMISSION

BIBLIOGRAPHIC DATA SHEET

SEE INSTRUCTIONS ON THE REVERSE

1. REPORT NUMBER (Assigned by TIDC, add Vol. No., if any)	LA-11117-MS NUREG/CR-4998
2. TITLE AND SUBTITLE	The Seismic Cateogry I Structures Program: Results for FY 1985
3. LEAVE BLANK	
4. DATE REPORT COMPLETED (MONTH / YEAR)	August 1987
5. AUTHOR(S)	Joel G. Bennett, Richard C. Dove, Wade E. Dunwoody, Charles R. Farrar, Peggy Goldman
6. DATE REPORT ISSUED (MONTH / YEAR)	December 1987
7. PERFORMING ORGANIZATION NAME AND MAILING ADDRESS (Include Zip Code)	Los Alamos National Laboratory Box 1663 Los Alamos, NM 87545
8. PROJECT/TASK/WORK UNIT NUMBER	
9. FIN OR GRANT NUMBER	A7221
10. SPONSORING ORGANIZATION NAME AND MAILING ADDRESS (Include Zip Code)	Division of Engineering Office of Nuclear Regulatory Research U.S. Nuclear Regulatory Commission Washington, DC 20555
11a. TYPE OF REPORT	Informal
b. PERIOD COVERED (Inclusive dates)	
12. SUPPLEMENTARY NOTES	

13. ABSTRACT (200 words or less)

In FY 1985 a new effort was begun to resolve an issue that became the "stiffness difference issue." This issue came about from reporting the results from testing both isolated shear walls and box-like shear deformation-dominated scale models that showed a consistent reduction in structural stiffness measured experimentally. This structural stiffness was different from that which would be calculated analytically at loads associated with operating basis earthquake levels. Several possible explanations were proposed for the experimental/analytical difference (most likely attributable to cracking of the concrete models). Possibilities are microcracking at very low loads, microconcrete effects, such as shrinkage cracks, unaccounted for dynamic effects in the analyses, and low stress level, low-cycle, fatigue degradation of microconcrete properties. A new configuration was proposed by the Technical Review Group (TRG) for this program and, in FY 1985, a prototype structure was designed. A 1/4-scale microconcrete model of the prototype structure was constructed and tested. This report details that investigation, but it does not report the resolution of the "stiffness difference" issue, an investigation that was ongoing at the end of FY 1985.

14. DOCUMENT ANALYSIS – a. KEYWORDS/DESCRIPTORS	
b. IDENTIFIERS/OPEN-ENDED TERMS	
15. AVAILABILITY STATEMENT	Unlimited
16. SECURITY CLASSIFICATION (This page)	Unclassified
(This report)	Unclassified
17. NUMBER OF PAGES	
18. PRICE	

Available from

Superintendent of Documents
U.S. Government Printing Office
Post Office Box 37082
Washington, D. C. 20013-7982

and

National Technical Information Service
Springfield, VA 22161

Los Alamos